

# Application of Plasma Enhanced Chemical Vapor Deposition for Fingerprint Resistance

Lei Wenwen, Chen Qiang, Qi Fengyang, Yang Lizhen, Liu Zhongwei, Wang Zhengduo

Beijing Institute of Graphic Communication, Beijing 102600, China

**Abstract:** SiO<sub>x</sub> and diamond-like carbon (DLC) coatings as the fingerprint resistance and corrosion resistance layers were deposited by capacitively coupled plasma (CCP)-enhanced chemical vapor deposition powered by radio frequency (RF-PECVD). In here hexamethyldisiloxane (HMDSO) as monomer for SiO<sub>x</sub> coating, C<sub>2</sub>H<sub>2</sub> as the carbon source for DLC growth precursor, and Ar as the dilution gas were utilized. The important factors affected fingerprint resistance was explored in detail. Besides, the corrosion resistant test on coatings and substrates were then examined by the potentiodynamic polarization measurement and salt-spray corrosion test, respectively. The chemical structure and composition of SiO<sub>x</sub> and DLC films were analyzed by FTIR, and the relationship between them and anti-corrosion property was discussed. The results show that the DLC coating demonstrates a better anti-fingerprint behavior than that of coated SiO<sub>x</sub>, especially in acidic solution environment.

**Key words:** SiO<sub>x</sub> and DLC coatings, CCP, fingerprint resistance, corrosion resistance

Fingerprint on commodities are always shown in daily life. Some products require no fingerprint and scratches remained on the surface, such as the surface of mobile phones, the decorative metals and glasses. As well known, there are grease and humidity on human being's fingers, and some of metal products are easily corroded in this environment. Besides, the surfaces are also frequently scratched during use. Thus, the surface treatment of metalwares is necessary to improve their corrosion resistance and wear resistance.

In this paper, we demonstrate the results of capacitively coupled plasma (CCP) enhanced chemical vapor deposition (PECVD) technology to prepare DLC and SiO<sub>x</sub> coatings on various substrates (such as silicon, copperplate, mobile phone covers). For exploring properties of the functional coatings, we characterized the structure, compound and morphology, corrosion resistance, wear resistance through Fourier transform infrared (FTIR), atomic force microscope (AFM), salt-spray corrosion test, electrochemistry corrosion test, and friction wear test, respectively.

## 1 Experiments

DLC and SiO<sub>x</sub> coatings were deposited separately in plasma setups which are illustrated in Fig.1a and 1b, respectively. They are capacitively coupled plasma with a radio frequency (RF, 13.56 MHz) power source, which the powered electrode is also as the substrate holder. During DLC deposition, the

carbon source acetylene (C<sub>2</sub>H<sub>2</sub>) and diluted Ar gas were flowed into the chamber from the top. For SiO<sub>x</sub> deposition, oxygen gas and hexamethyldisiloxane (HMDSO) were used as oxidant and monomer, respectively, and argon was utilized as a diluted gas. The discharge parameters, such as the acetylene

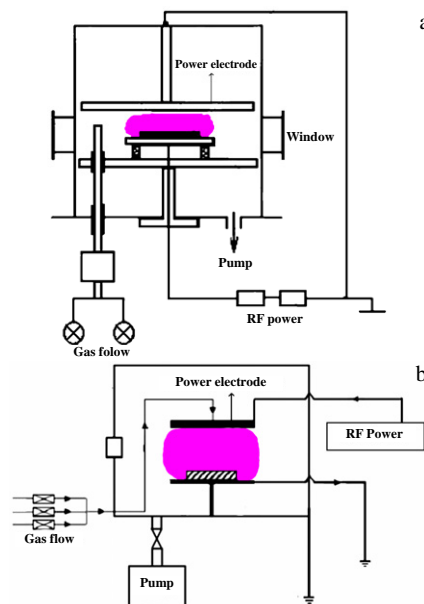


Fig.1 Schematic diagram of the PECVD reactor system: (a) for DLC deposition; (b) for SiO<sub>x</sub> deposition

Received date: May 25, 2011

Foundation item: Beijing Natural Science Foundation (No.1112012), KM201110015008, KM201010015005 and PHR20110516.

Corresponding author: Chen Qiang, Ph. D., Professor, Laboratory of Plasma Physics and Material, Beijing Institute of Graphic Communication, Beijing 102600, P. R. China, Tel: 0086-10-60261099, E-mail: lppmchenqiang@hotmail.com

concentration, the rate of HMDSO and O<sub>2</sub>, the deposition time and discharge power were varied for the purpose to study the influence on deposited coating properties. The deposition conditions were summarized in table 1.

The samples were cleaned ultrasonically in ethanol solution for 5 min and then rinsing with deionized (DI) water for several minutes before deposition. The structural components of the coatings were analyzed by FTIR spectroscopy (FTIR-8400, Shimadzu, Japanese). The film morphologies were analyzed by atomic force microscope (AFM, CSPM 3000, Ben Yuan, China), and the average roughness was obtained with flattening corrections of 10.0×10.0 μm<sup>2</sup> scan. The friction-wear resistance was measured by Tribometer (WTM-1E, Institute of Chemical Physics, Chinese Academy of Sciences). The corrosion resistance test was performed based on ASTM B117 1788 and GBT10125 as standard referenced test with NaCl solution, and copper accelerated acetic acid salt-spray test solution (pH 3.1~3.3) was carried out at 35 °C for 6 h in salt-spray corrosion tester (07-7004-M, China). The angle of sample placement is 20°, and the test chamber saturation temperature was 50 °C. When the measurement was finished, the samples were dried in the air for 0.5~1 h, then cleaned in flowing water (< 40 °C), and finally dried with blowing N<sub>2</sub>. Electrochemical experiments were carried out with a standard three-electrode system. A saturated calomel electrode (SCE) was used as the reference electrode with a platinum counter electrode. The corrosion resistance was examined in 5% NaCl solution at 25 °C (pH 7). Potentiodynamic polarization experiments was started after the specimen was immersed in the experimental solution for 2000 s under open-circuit conditions and performed at a rate of 0.5 mV/s.

## 2 Results and Discussion

### 2.1 FTIR analysis

#### 2.1.1 FTIR of DLC coatings

Fig.2 displays the typical FTIR spectra of deposited DLC coatings. In Fig.2a, the obvious absorption peak at around 1400 cm<sup>-1</sup>, assigned to the C-CH<sub>3</sub> groups (sp<sup>3</sup>) stretching vibration, and the absorption peaks in the range of 3000-2800 cm<sup>-1</sup> for C-H<sub>n</sub> stretching vibrations clearly illustrate that the film consists of DLC component. Closely analyzing the spectrum one can note that the DLC film is mostly composed of sp<sup>3</sup> hybridized bonding and has high bonded hydrogen content<sup>[1,2]</sup>. Otherwise, owing to C-H stretching vibrations under 3000 cm<sup>-1</sup>, it is considered that carbon atoms are at a saturation state in the film. The strong absorption peak at

**Table 1 Deposition conditions of DLC and SiO<sub>x</sub> by PECVD**

| Deposition condition   | DLC              | SiO <sub>x</sub> |
|------------------------|------------------|------------------|
| Base pressure/Pa       | 5                | 2                |
| Working pressure/Pa    | 20               | 20               |
| Substrate temperature/ | Room temperature |                  |

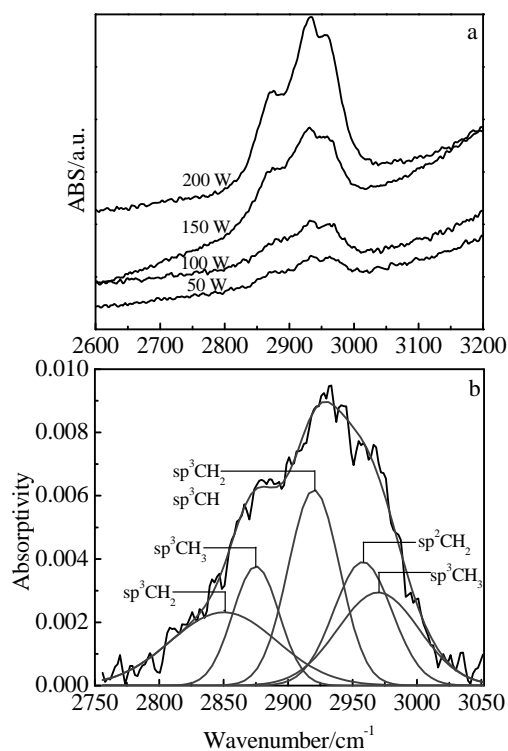


Fig.2 FTIR of deposited DLC films: (a) characteristic peak of DLC films and (b) the results of fitting peaks in Gaussian mode

3410-3300 cm<sup>-1</sup> was O-H vibration mode following DLC film post-reaction. Fig.2b displays the results of fitting peaks in Gaussian mode at discharge power 150 W. The spectrum reveals the coatings are a typical polymer-like structure: the sp<sup>3</sup> CH<sub>3</sub> bonding types at 2875 cm<sup>-1</sup> and 2970 cm<sup>-1</sup> strongly dominate the spectrum, but the clear contribution from sp<sup>2</sup> CH<sub>2</sub> at 2958 cm<sup>-1</sup> definitely means it is polymer-like material based on the ascription by Dischler<sup>[3]</sup>.

#### 2.1.2 FTIR of SiO<sub>x</sub> coatings

The structures of SiO<sub>x</sub> coatings at different discharge powers and the ratios of O<sub>2</sub> and HMDSO measured by FTIR are exhibited in Fig.3. From Fig.3a, one can see there are absorption peaks at around 1060-1070 cm<sup>-1</sup>, 805-810 cm<sup>-1</sup> and 480-490 cm<sup>-1</sup>, which are Si-O-Si groups stretching vibration and bending vibration. The discharge power has no obvious effect on the structure of SiO<sub>x</sub>. However, in Fig.3b, one can find that different ratios of O<sub>2</sub> and HMDSO change the structures of SiO<sub>x</sub>. The increased concentration of oxygen and the broadness of the peaks in the FTIR spectra, indicate that complete ring fragmentation occurs to a large extent in the plasma, leading to the deposition of SiCOH films from HMDSO. And in this situation, the network structure is gained, and SiO<sub>2</sub> would be formed<sup>[4]</sup>.

### 2.2 Friction coefficient

Fig.4 shows the friction coefficient at different concentrations of C<sub>2</sub>H<sub>2</sub>, discharge powers and deposition time measured with load of 50 g, rotational speed at 1000 r/min, rotational

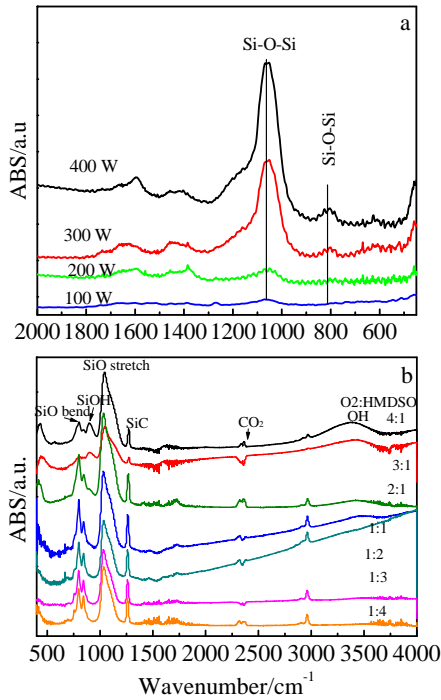


Fig.3 FTIR of deposited SiO<sub>x</sub> at variety of (a) discharge powers and (b) ratios of O<sub>2</sub> and HMDSO.

diameter of 4 mm. The friction coefficient of blank glass slide

is 0.842, and with the DLC coatings that are sharply decreased to 0.18, i.e. DLC coatings could improve the friction-wear resistance properties. The most effective results are gained when the Ar concentration is increased and the discharge power is relatively high. This is because concentration of Ar is connection with the number of sp<sup>2</sup> in DLC films, i.e. graphite concentration, which improves the friction resistance<sup>[5]</sup>.

**2.3 Atomic force microscope (AFM) analysis**

To investigate the morphologies of the deposited coatings on substrates, the AFM observation of films were carried out. The data derived from AFM images, the average roughness (R<sub>a</sub>), were obtained with flattening corrections of (10.0×10.0) μm<sup>2</sup> scan as Fig.5 shows.

From Fig.5, we can see the deposited films are smooth, and the particles are uniform. The roughness average (R<sub>a</sub>) are 0.892 and 0.783, respectively. It is well known that the smooth surface is favourable for anti-fingerprint behaviour.

**2.4 Salt-spray test of DLC and SiO<sub>x</sub> coatings**

Fig.6 displays results of the salt-spray corrosion test of the deposited DLC coatings at different thicknesses. The thicknesses are 25, 75, and 150 nm from Fig.6a to 6c, respectively. In these images, the light color corresponds to the corroded sites. According to the standards GB/T6461-2002, the corrosive rate is obtained from following equation:

$$R_p=3(2-\lg A) \tag{1}$$

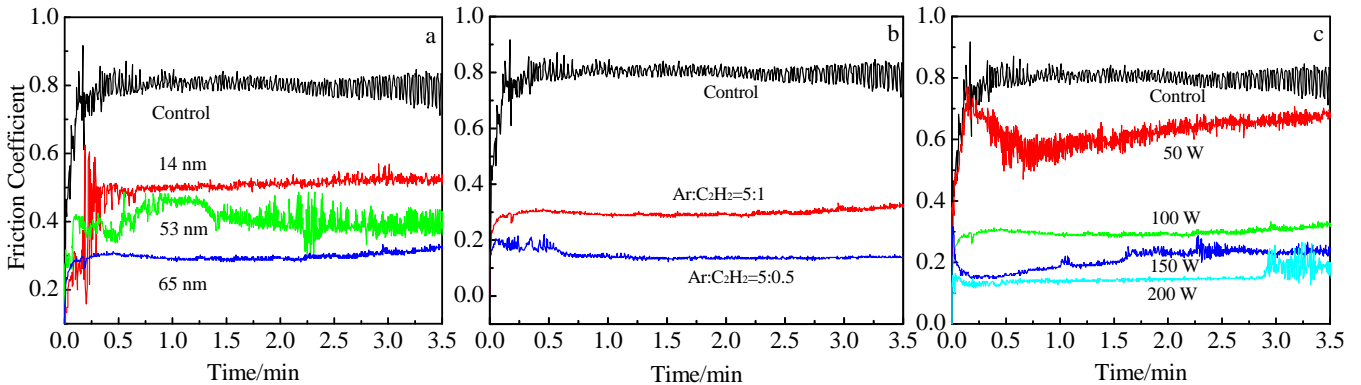


Fig.4 Friction-wear resistance of deposited DLC coatings at variety of (a) thickness, (b) concentrations of Ar, and (c) discharge powers

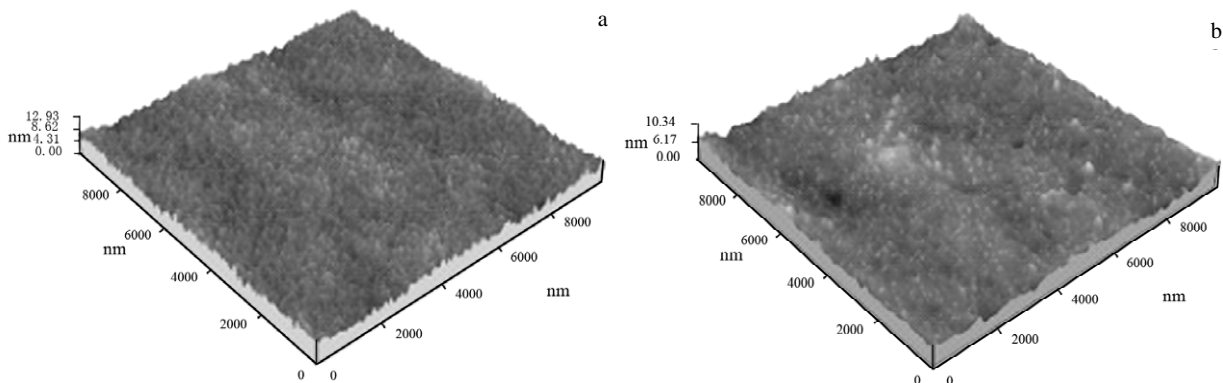


Fig.5 AFM images of the coating under (a) 100 W, Ar:C<sub>2</sub>H<sub>2</sub>=5:1, 60 min, 10 Pa and (b) 150 W, Ar:C<sub>2</sub>H<sub>2</sub>=5:1, 60 min, 10 Pa

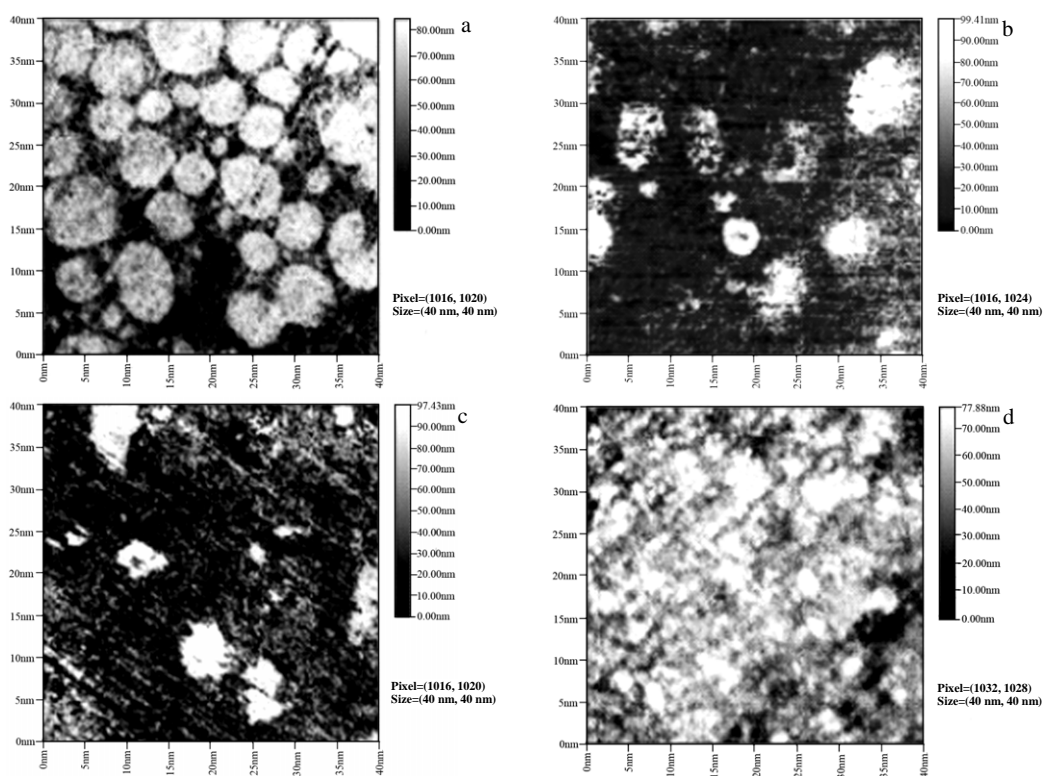


Fig.6 SEM images of salt-spray resistance test of DLC coatings on copper substrates at different thicknesses: (a) 25 nm, (b) 75 nm, (c) 150 nm, and (d) blank copper sample

where  $R_p$  is the protective rating,  $A$  is the percent of corroded square meter in total area. From Image 4.6 software,  $A$  could be obtained, and the calculated results are summarized in Table 2.

From the data, one can see that the protective rating is obvious higher as the thicknesses of DLC coatings are larger. This means that the thicker the DLC films is, the better the salt-spray resistance is.

Fig.7 shows the salt-spray corrosion test results relevance to the concentrations of Ar. The calculated results are summarized in Table 3.

From these images and calculated data, we can assume that the higher concentration of Ar might influence the ratio of  $sp^3/sp^2$ , which dominates corrosion resistance of deposited films.

## 2.5 Electrochemical Corrosion

### 2.5.1 Electrochemical corrosion of DLC coatings

Fig.8 shows the potentiodynamic polarization curves of the

**Table 2 Corrosion square meter percent ( $A$ ) and protective rating ( $R_p$ ) of corroded DLC films with different thicknesses**

| DLC thickness/nm | $A/\%$ | $R_p$ |
|------------------|--------|-------|
| 0                | 53     | 0     |
| 25               | 42     | 1     |
| 75               | 22     | 2     |
| 150              | 8      | 3     |

DLC coated copper in 3.5% NaCl solution. The corrosion behavior of the uncoated sample is also included in this figure for comparison. The corrosion potential ( $E_{corr}$ ) and the passive current density ( $I_p$ ) of the DLC uncoated and coated copper obtained from Fig.8 are listed in Table 4. It can be seen from Table 4 that the corrosion resistance of the copper is improved due to the coating of DLC films, and corrosion resistance of the DLC films on copper is increased with increasing of the thickness of DLC films, but then decreases with further increasing of Ar concentration.

The improvement of the corrosion resistance of the coated sample may be attributed to the reduced electrical conductivity caused by the chemical inertness of the DLC films in comparison to the uncoated sample. The low electrical conductivity of the DLC films reduces the electron transport and the exchange of electrical charges at the samples surface, which is necessary for the electrochemical corrosion<sup>[6]</sup>. Combination the ratio of  $sp^3/sp^2$  and the electrochemical corrosion behavior listed in Table 4 for the DLC films, it can be readily observed that these two parameters are agreed well with each other. The reason that the corrosion resistance of the DLC films depending on the structure may be because the electrical conductivity is closely related to the  $sp^3/sp^2$  ratio, correspondingly, the higher the  $sp^3/sp^2$  ratio is, the lower the electrical conductivity is. Thus, the DLC coated sample with higher  $sp^3/sp^2$  ratio possesses higher corrosion resistance<sup>[7]</sup>.

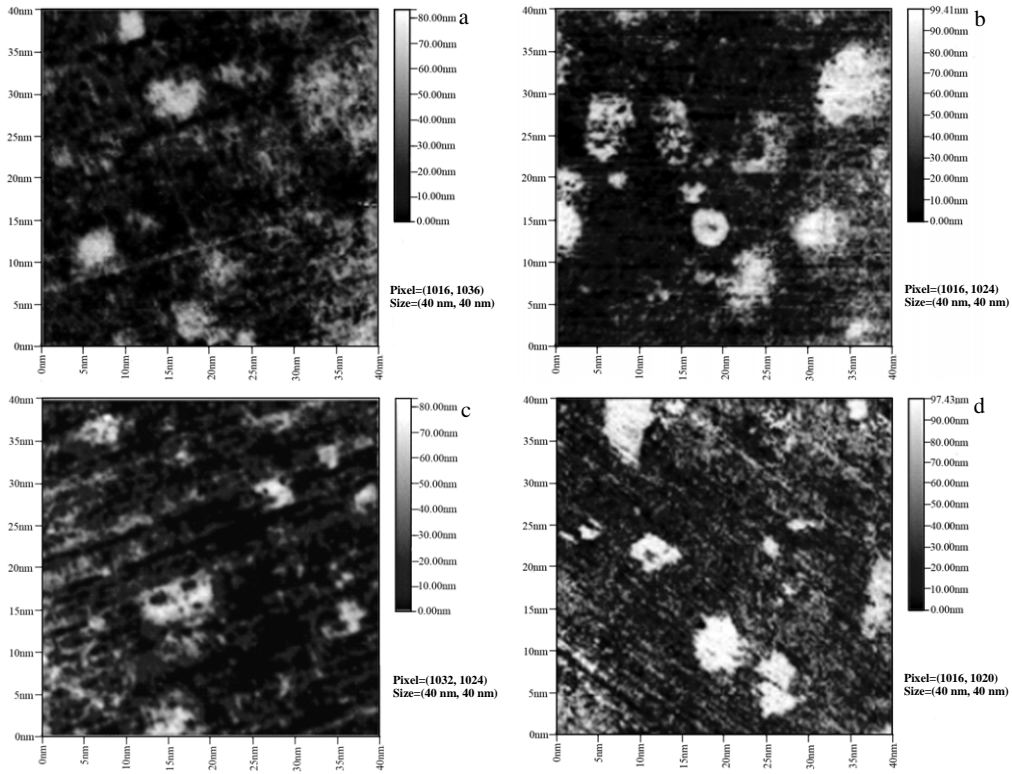


Fig.7 SEM images of salt-spray resistance test in different concentrations of Ar: (a) Ar:C<sub>2</sub>H<sub>2</sub>=5:1, DLC thickness=75 nm; (b) Ar:C<sub>2</sub>H<sub>2</sub>=5:2, DLC thickness=75 nm; (c) Ar:C<sub>2</sub>H<sub>2</sub>=5:1, DLC thickness=150 nm; (d) Ar:C<sub>2</sub>H<sub>2</sub>=5:2, DLC thickness=150 nm

**Table 3 Corrosion square meter percent (A) and protective rating (R<sub>P</sub>) of corroded DLC films with different concentrations of Ar**

| Ar concentration                      | Thickness of DLC/nm | A/% | R <sub>P</sub> |
|---------------------------------------|---------------------|-----|----------------|
| Ar:C <sub>2</sub> H <sub>2</sub> =5:1 | 75                  | 33  | 1              |
|                                       | 150                 | 11  | 2              |
| Ar:C <sub>2</sub> H <sub>2</sub> =5:2 | 75                  | 22  | 2              |
|                                       | 150                 | 8   | 3              |

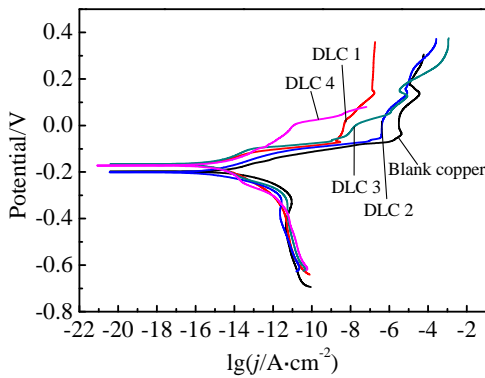


Fig.8 Potentiodynamic polarization curves of the uncoated and DLC coated copper (DLC1-Ar:C<sub>2</sub>H<sub>2</sub>=5:1, thickness=75 nm; DLC2-Ar:C<sub>2</sub>H<sub>2</sub>=5:1, thickness=150 nm; DLC3-Ar:C<sub>2</sub>H<sub>2</sub>=5:2, thickness=75 nm; DLC4-Ar:C<sub>2</sub>H<sub>2</sub>=5:2, thickness=150 nm)

### 2.5.2 Electrochemical corrosion of SiO<sub>x</sub> coatings

The electrochemical corrosion results of SiO<sub>x</sub> coatings are shown in Fig.9. It can be seen from this image that

**Table 4 Results of the uncoated and DLC coated copper derived from the anodic polarization curves**

| Sample | E <sub>corr</sub> /mV | I <sub>p</sub> /A·cm <sup>-2</sup> |
|--------|-----------------------|------------------------------------|
| Copper | -200                  | 1.2×10 <sup>-3</sup>               |
| DLC1   | -180                  | 4.04×10 <sup>-4</sup>              |
| DLC2   | -200                  | 4.06×10 <sup>-4</sup>              |
| DLC3   | -180                  | 3.60×10 <sup>-4</sup>              |
| DLC4   | -180                  | 3.80×10 <sup>-4</sup>              |

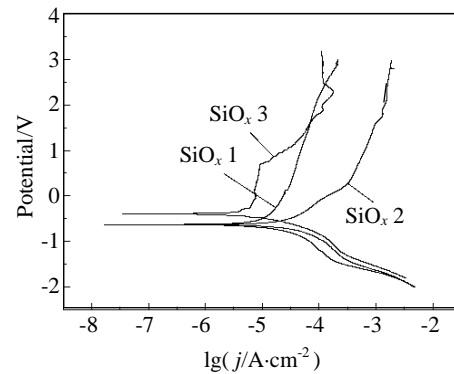


Fig.9 Potentiodynamic polarization curves of the uncoated and SiO<sub>x</sub> coated copper (SiO<sub>x</sub>1- O<sub>2</sub>:HMDSO=4:1; SiO<sub>x</sub>2- O<sub>2</sub>:HMDSO=3:1; SiO<sub>x</sub>3- O<sub>2</sub>:HMDSO=2:1)

corrosion resistance of the  $\text{SiO}_x$  coatings on copper is increased with the ratio of  $\text{O}_2$  and HMDSO. From Fig.3, as the ratio is larger, the network structure of deposited films is formed. Thus, demonstrate the coatings have more protective behavior.

### 3 Conclusions

1) The deposited DLC films with  $\text{C}_2\text{H}_2$  as carbon source, Ar as diluted gas by PEVCVD, can sharply improve the protective properties of substrates, including salt-spray resistance, electrochemical resistance, and friction-wear resistance.

2) These properties are closely related to  $\text{sp}^3/\text{sp}^2$  ratio of DLC films. The higher the  $\text{sp}^3/\text{sp}^2$  ratio is, the better the corrosion resistance is; and the lower the  $\text{sp}^3/\text{sp}^2$  ratio is, the better the friction-wear resistance is.

3)  $\text{SiO}_x$  films can also improve corrosion resistance of substrates in here, the higher the oxygen concentration is, the better the corrosion resistance is.

### References

- 1 Li W Y, Liao H L, Douchy G et al. *Mater Des*[J], 2007, 28: 2129
- 2 Dischler B, Bubenzer A, Koidl P. *Applied Physics Letter*[J], 1983, 42: 636
- 3 Liu Dongping, Liu Yanhong, Chen Baoxiang. *Chinese Physics B*[J], 2006, 15:575
- 4 Dischler B. *Proceedings of European Material Research Society Meeting*[C]. Paris: Les Editions de Physique, 1987: 189
- 5 Alfred Grill, Deborah A Neumayer. *Journal of Applied Physic*[J], 2003, 94: 6697
- 6 Yang Li, Chen Qiang. *National Electric Charge and Ion Beam Academic Conference*[C]. Harbin: Electric Engineering Press, 2008: 146
- 7 Annett D R, Schurer C, Irmer G et al. *Surface Coating Technology*[J], 2004, 177: 830
- 8 Sui J H, Gao Z Y, Cai W et al. *Materials Science and Engineering A*[J], 2007, 454: 47